Water Splitting on Composite Plasmonic-Metal/Semiconductor Photoelectrodes: Evidence for Selective Plasmon-Induced Formation of Charge Carriers near the Semiconductor Surface

David B. Ingram and Suljo Linic*

Department of Chemical Engineering, University of Michigan, Ann Arbor, Michigan 48109, United States

S *Supporting Information*

ABSTRACT: A critical factor limiting the rates of photocatalytic reactions, including water splitting, on oxide semiconductors is the high rate of charge-carrier recombination. In this contribution, we demonstrate that this issue can be alleviated significantly by combining a semiconductor photocatalyst with tailored plasmonic-metal nanostructures. Plasmonic nanostructures support the formation of resonant surface plasmons in response to a photon flux, localizing electromagnetic energy close to their surfaces. We present evidence that the interaction of localized electric fields with the neighboring semiconductor allows for the selective formation of electron/hole (e^-/h^+) pairs in the near-surface region of the semiconductor. The advantage of the formation of e^-/h^+ pairs near the semiconductor surface is that these charge carriers are readily separated from each other and easily migrate to the surface, where they can perform photocatalytic transformations.

The efficient conversion of solar energy into fuels through the photochemical splitting of water to form H_2 and O_2 is of critical importance for the development of a sustainable energy future. It has been demonstrated that various oxide semiconductors are active photocatalysts for this reaction.[1] A crucial obstacle limiting the efficiency of almost every oxide semiconductor photocatalyst is the high rate of charge-carrier recombination.[2] The high charge-carrier recombination rate is the consequence of the discrepancy between the relatively large penetration depth of photons and the short mean free paths of charge carriers, which stipulates that a majority of the charge carriers are lost to recombination before they can reach the semiconductor surface and perform photochemical reactions. Attempts to address this problem have mainly centered on controlling the photocatalyst structure to maximize photon absorption while minimizing the distance charge carriers travel before reaching the surface.[3]

In this contribution, we demonstrate that the recombination problem can be alleviated significantly by combining an oxide semiconductor photocatalyst with tailored plasmonic-metal nanostructures. Plasmonic nanostructures support the formation of resonant surface plasmons (SPs) in response to a photon flux, localizing electromagnetic (EM) energy close to their surfaces.[4] We present evidence that the interaction of localized electric fields with a neighboring semiconductor allows for the selective formation of electron/hole (e^-/h^+) pairs in the near-surface region of the

semiconductor. The charge carriers formed near the semiconductor surface reach the active surface sites more readily than charge carriers formed in the bulk. This results in a decrease in the charge-carrier recombination rate and increases the water splitting rate on composite photocatalysts that contain a plasmonic metal and a semiconductor.

Our conclusions were obtained in studies of the water splitting reaction under broadband visible-light illumination in a conventional three-electrode photoelectrochemical cell. A few previous examples of similar photocatalysts have focused on photoinduced exothermic reactions such as photo-oxidation of methylene blue or other organic compounds.[5] The reversible nature of the water splitting reaction makes this process mechanistically different and potentially more sensitive to local surface concentrations of charge carriers than the exothermic photoinduced reactions.

The electrolyte was 1 M KOH, and the reference electrode was Hg/HgO. A Pt wire was used as the counter electrode for the H_2 evolution half-reaction, and a 0.3 V bias was applied in all experiments to assist in the evolution of H_2 at the Pt counter electrode (see the Supporting Information for experimental details). The photoelectrode for the O_2 evolution reaction was nitrogen-doped TiO_2 (N-TiO_2) or a composite material containing Ag nanocubes (edge length 118 ± 25 nm) or Au spheres (diameter 24.5 ± 4.5 nm) along with N-TiO_2. Unlike native TiO_2, N-TiO_2 is optically active in the visible region of the solar spectrum, as shown in Figure 1b.[6] We focused on this size and shape of the Ag nanoparticles, since these nanostructures exhibit intense surface plasmon resonance (SPR) in the region where the N-TiO_2 semiconductor absorbs visible light (i.e., 400–500 nm; see Figure 1b). This is illustrated in Figure 1a, where the extinction efficiencies (averaged over the 400–500 nm source wavelength) are shown. Extinction efficiency is defined as the extinction cross section, calculated using finite-difference time-domain (FDTD) simulations,[7] divided by the geometric cross section. The extinction is the consequence of the formation of resonant Ag SP states. The Au/N-TiO_2 photoelectrodes were used in control experiments. The conductivity and electronic structure of Au are similar to those of Ag, but the Au SPR is red-shifted relative to that of Ag and does not overlap significantly with N-TiO_2 absorption spectrum, as shown in Figure 1.

N-TiO_2 was synthesized by heating TiO_2 particles (~20 nm diameter) in the presence of NH_3.[6b] The Ag nanocubes and Au spheres were synthesized using a previously reported modified polyol process.[8] The metal nanostructures were coated with non-conducting organic stabilizer molecules [poly(vinylpyrrolidone)
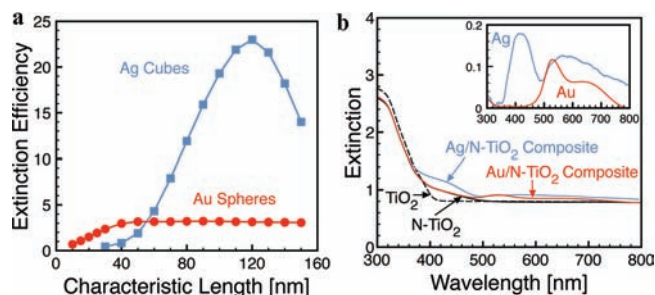
Figure 1. (a) Extinction efficiencies (extinction cross section divided by geometric cross section) averaged over wavelengths of 400−500 nm for Ag cubes and Au spheres as functions of particle size (cube edge length or sphere diameter). These were calculated using FDTD optical simulations (see the Supporting Information). (b) UV−vis extinction spectra of TiO_2, $N-TiO_2$, $Ag/N-TiO_2$ and $Au/N-TiO_2$ samples. The inset shows difference spectra for Ag and Au (i.e., the $Ag/N-TiO_2$ or $Au/N-TiO_2$ spectrum minus the $N-TiO_2$ spectrum).
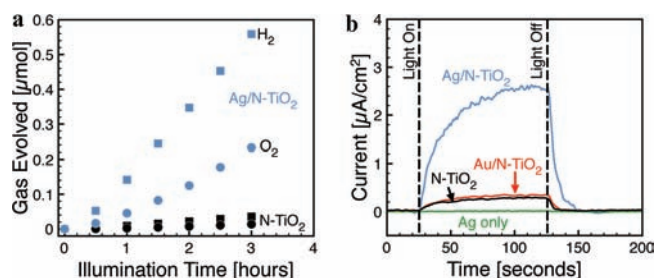

Figure 2. (a) H_2 (■) and O_2 (●) production upon visible illumination of $N-TiO_2$ (black symbols) and $Ag/N-TiO_2$ (blue symbols) photocatalysts, as measured by mass spectrometry. (b) Photocurrent responses (per macroscopic electrode area) upon illumination with a broadband visible light source (400−900 nm).

Figure 3. (symbols) Photocurrent enhancement for $Ag/N-TiO_2$ composite (photocurrent for $Ag/N-TiO_2$ divided by that for $N-TiO_2$) as a function of excitation wavelength. (solid curve) Ag nanocube spectrum (difference spectrum for $Ag/N-TiO_2$ from the Figure 1b inset). While large enhancements are observed at energies lower than the $N-TiO_2$ absorbance (i.e., >500 nm), the absolute reaction rates at these wavelengths are very small (see Figure S5 in the Supporting Information).

(PVP)]. These stabilizer molecules play a critical role in separating the metal and semiconductor particles and limiting Förster energy transfer between the semiconductor and the metal. This is discussed in more detail below. A more detailed description of the photocatalyst preparation can be found in Supporting Information.

The composite photoelectrodes were physical mixtures of Ag and $N-TiO_2$ ($Ag/N-TiO_2$) or Au and $N-TiO_2$ ($Au/N-TiO_2$). The metal loading was 5% by weight with respect to the semiconductor. The photoelectrodes were supported on an inert conductive substrate (glass coated with indium tin oxide). The mass, volume, and surface area of $N-TiO_2$ were constant in all of the experiments. The resulting photoelectrode films were ∼0.75 μm thick (as measured by ellipsometry). UV−vis extinction spectra of the photoelectrode samples are shown in Figure 1b. The figure inset shows the differences in extinction between the composite materials and the samples containing $N-TiO_2$ only. The difference is due to the light-induced resonant formation of SP states on the Au and Ag nanoparticles.

Figure 2a shows that upon illumination of the photoelectrodes with a broadband visible source (400−900 nm, ∼500 mW/cm², spectral peak at 580 nm), stoichiometric amounts of H_2 and O_2 were produced, suggesting the overall splitting of water. The current response is shown in Figure 2b. The photocurrent is proportional to the water splitting reaction rate: transforming two molecules of water into $2H_2$ and O_2 produces four electrons that flow through the external circuit. Figure 2b shows that the addition of plasmonic Ag nanoparticles to $N-TiO_2$ increases the
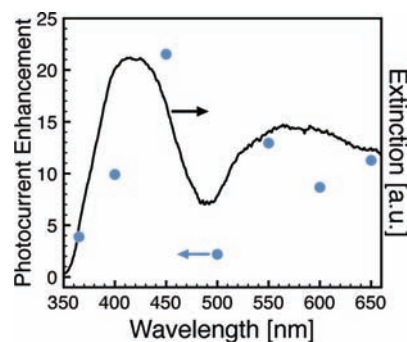
visible-light photocurrent by a factor of ∼10. On the other hand, the addition of Au nanoparticles has only a small effect on the photocurrent.

Figure 3 shows the photocurrent enhancement for the $Ag/N-TiO_2$ photoelectrode (calculated as the photocurrent for $Ag/N-TiO_2$ divided by that for $N-TiO_2$) as a function of source wavelength. Optical filters were used to modulate the wavelength of the broadband visible source. The figure shows that the enhancement depends strongly on the source wavelength and that it qualitatively tracks the intensity of the Ag UV−vis extinction (also shown in Figure 3). Since the Ag extinction is a consequence of the excitation of Ag SP states, the qualitative mapping between the rate enhancement and the Ag extinction suggests that the Ag plasmons are responsible for the observed rate enhancement.

We previously investigated the interactions between excited plasmonic-metal particles coated with nonconductive molecules and a nearby semiconductor in a nonreactive environment. These studies showed that for these systems, the presence of the organic layer prevents direct electron transfer; instead, energy is transferred from the metal SPs to the semiconductor in a radiative process, increasing the overall concentration of charge carriers in the semiconductor[5d] (please consult the Supporting Information for a more detailed discussion of alternative mechanisms).

This energy-transfer mechanism is further supported by a comparison of the water splitting performance of composites containing Ag and Au nanostructures. Unlike the $Ag/N-TiO_2$ composites, the photoelectrodes containing Au did not show significant rate enhancements (see Figure 2b). The only significant difference between the optical properties of Ag and Au is that the Au SPR is red-shifted relative to that of the Ag cubes. Figure 1b shows that the Au nanostructures support SPR at wavelengths above 500 nm. This energy of the Au SPR is insufficient to lead to the formation of e^-/h^+ pairs in $N-TiO_2$ in the radiative energy transfer process, as $N-TiO_2$ absorbs only below ∼500 nm. The different performance of $Ag/N-TiO_2$ and $Au/N-TiO_2$ provides additional evidence that the role of the metal in this system is not to promote the conduction of charge carriers in the composite photoelectrodes.

It is important to analyze how this energy transfer from plasmonic Ag nanostructures results in such a dramatic increase in the reaction rate. To address this issue, we analyze the interaction of the Ag SP
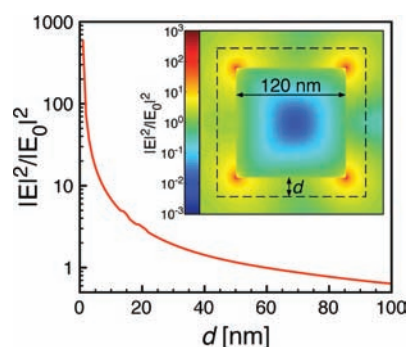
5203

dx.doi.org/10.1021/ja200086g |*J. Am. Chem. Soc.* 2011, 133, 5202–5205

Figure 4. Average electric field enhancement around a Ag cube with an edge length of 120 nm as a function of the distance d from the cube, as calculated using FDTD simulations. Inset: Local enhancement of the electric field calculated from an FDTD simulation of a 120 nm Ag cube in water.

Figure 5. Photocurrent as a function of broadband visible-light intensity for N-TiO$_2$ and composite Ag/N-TiO$_2$ samples. Ag/N-TiO$_2$ exhibits approximately a linear (first-order) dependence on the light intensity, while N-TiO$_2$ exhibits an approximately half-order dependence.

states with a flux of resonant source photons. For large Ag nanostructures (characteristic length above ∼50 nm), this interaction leads to a very efficient scattering of resonant photons by the nanostructures.[4] Therefore, for large Ag nanoparticles, the extinction by the Ag/N-TiO$_2$ composites is a superposition of the direct absorption by N-TiO$_2$ (leading to e$^-$/h$^+$ pairs) and mainly scattering from the Ag structures (Figure 1b). The scattering of photons by Ag increases the average photon path length in the composites, causing an increased rate of e$^-$/h$^+$ pair formation in N-TiO$_2$. Here, Ag would essentially be acting as a mirror: some resonant photons that are not absorbed by N-TiO$_2$ upon their first pass through the composite material could be scattered by Ag, effectively giving those photons multiple passes through the system. The scattering effect can be isolated and quantified by measuring the increase in photon extinction in the sample due to the addition of Ag particles. If we assume that every photon that is scattered by Ag is absorbed by N-TiO$_2$ and converted to an e$^-$/h$^+$ pair, we would expect a one-to-one mapping between the rate enhancement and the enhancement in the number of scattered photons (related but not equal to the difference spectrum in Figure 3). On the basis of an analysis of the UV−vis extinction spectra in Figure 1b, we estimate that at 400−500 nm there is at most an increase of ∼25% in the number of photons absorbed in the Ag/N-TiO$_2$ sample relative to N-TiO$_2$. This increase in absorbed photons is insufficient to explain the much larger observed enhancements in the reaction rate.

In addition to efficient photon scattering, the formation of resonant SP states results in an enhancement of local electric fields in the neighborhood of the Ag nanostructures.[4] This is illustrated in Figure 4, which shows the FDTD-calculated field enhancements from a 120 nm Ag cube in water. When a semiconductor is brought into the proximity of Ag, it encounters these intense electric fields. This process results in the rapid formation of e$^-$/h$^+$ pairs in the semiconductor. An important feature of the electric fields is that they are spatially nonhomogenous, with the highest field strength in the proximity of the nanostructures. This suggests that SP-induced e$^-$/h$^+$ pair formation should be greatest in the part of the semiconductor that is the closest to Ag, i.e., near the surface of the semiconductor particles (essentially at the semiconductor−liquid interface). The advantages of forming e$^-$/h$^+$ pairs near the semiconductor surface rather than in the bulk are that (i) the charge carriers are readily separated from each other under the influence of the surface potential and (ii) the charge carriers have a shorter distance to migrate in order to reach the surface, where they can perform
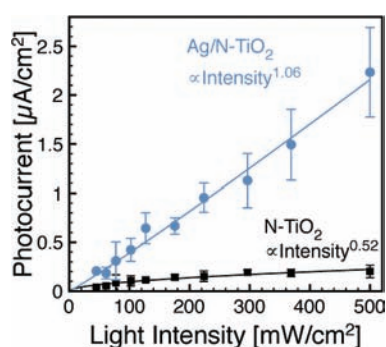
photocatalytic transformations. This effectively means that the probability of photoreaction is enhanced relative the probability of charge-carrier recombination. It should be mentioned that the optimal distance between a semiconductor and a plasmonic nanostructure is also affected by Förster energy transfer from the semiconductor to the metal.[9] In the photoelectrodes used herein, the organic PVP layer represents a buffer that keeps the two nanostructures at a finite distance from each other without physically touching, providing an environment where the negative effect of the Förster energy transfer is diminished.

To further test the hypothesis that very intense local electric fields lead to increased rates of e$^-$/h$^+$ pair formation at the semiconductor surface, resulting in large rate enhancements, we measured the rate of the water splitting reaction as a function of the intensity of broadband visible illumination. Figure 5 shows that N-TiO$_2$ exhibits approximately half-order dependence on the light intensity, while the composite Ag/N-TiO$_2$ exhibits approximately first-order dependence. If we assume that the rate of oxygen evolution on the semiconductor is linearly dependent on the surface concentration of h$^+$, then Figure 5 shows that the surface concentration of h$^+$ follows first- and half-order intensity dependences in Ag/N-TiO$_2$ and N-TiO$_2$, respectively. The observed linear dependence of the surface concentration of h$^+$ on the light intensity for Ag/N-TiO$_2$ is another indication that charge carriers are formed close to the semiconductor surface in the composite Ag/N-TiO$_2$ system. We note that it has been shown previously in surface-science measurements that the surface h$^+$ concentration for charge carriers formed in the bulk of TiO$_2$ shows a half-order dependence on light intensity, whereas the surface concentration of h$^+$ for charge carriers formed in the surface layers of TiO$_2$ depends linearly on light intensity.[10] In those measurements, the surface-specific formation of charge carriers was accomplished by using a flux of energetic electrons with penetration depths significantly smaller than those of photons.[10b] The difference in intensity dependence was attributed to the fact that charge carriers formed in the bulk are lost mainly through the process of e$^-$/h$^+$ recombination (exhibiting a half-order dependence on the intensity), while the charge carriers formed close to the surface of the semiconductor mainly decayed in their reaction with surface trap states (exhibiting a first-order dependence on the light intensity).

In conclusion, we have demonstrated that plasmonic Ag nanostructures can be employed as building blocks to create composite plasmonic-metal/semiconductor photoelectrocatalysts that exhibit enhanced water splitting performance relative to the semiconductor

alone. Our experiments and simulations have shown that the enhancement can be attributed to the formation of intense electric fields at the Ag particle surface, which increase the rate of formation of e^-/h^+ pairs at the nearby N-TiO$_2$ particle surface (i.e., at the semiconductor—liquid interface). The advantage of the formation of e^-/h^+ pairs near the semiconductor surface is that these charge carriers are readily separated from each other and easily migrate to the surface, where they can perform photocatalytic transformations. The ability to tune the size and shape of plasmonic metal nanoparticles and thereby control the energy and intensity of the SPR offers a great deal of flexibility in the design of efficient composite plasmonic-metal/semiconductor photocatalysts. In addition to the critical importance of the size and shape of the plasmonic nanostructures, the proximity of the semiconductor and metal building blocks is another important design parameter.

■ ASSOCIATED CONTENT

Ⓢ **Supporting Information.** Detailed synthesis, sample preparation, and experimental and simulation methods. This material is available free of charge via the Internet at http://pubs.acs.org.

■ AUTHOR INFORMATION

Corresponding Author
linic@umich.edu

■ ACKNOWLEDGMENT

■ REFERENCES

(1) (a) Fujishima, A.; Honda, K. *Nature* **1972**, *238*, 37. (b) Cesar, I.; Kay, A.; Gonzalez, J. A.; Grätzel, M. *J. Am. Chem. Soc.* **2006**, *128*, 4582.

(2) (a) Linsebigler, A. L.; Lu, G.; Yates, J. T., Jr. *Chem. Rev.* **1995**, *95*, 735. (b) Fujishima, A.; Zhang, X.; Tryk, D. A. *Surf. Sci. Rep.* **2008**, *63*, 515.

(3) (a) Mor, G. K.; Shankar, K.; Paulose, M.; Varghese, O. K.; Grimes, C. A. *Nano Lett.* **2005**, *5*, 191. (b) Zhu, K.; Neale, N. R.; Miedaner, A.; Frank, A. J. *Nano Lett.* **2007**, 7, 69.

(4) (a) El-Sayed, M. A. *Acc. Chem. Res.* **2001**, *34*, 257. (b) Kelly, K. L.; Coronado, E.; Zhao, L. L.; Schatz, G. C. *J. Phys. Chem. B* **2003**, *107*, 668.

(5) (a) Tian, Y.; Tatsuma, T. *J. Am. Chem. Soc.* **2005**, *127*, 7632. (b) Awazu, K.; Fujimaki, M.; Rockstuhl, C.; Tominaga, J.; Murakami, H.; Ohki, Y.; Yoshida, N.; Watanabe, T. *J. Am. Chem. Soc.* **2008**, *130*, 1676. (c) Kowalska, E.; Abe, R.; Ohtani, B. *Chem. Commun.* **2009**, 241. (d) Christopher, P.; Ingram, D. B.; Linic, S. *J. Phys. Chem. C* **2010**, *114*, 9173. (e) Mori, K.; Kawashima, M.; Che, M.; Yamashita, H. *Angew. Chem., Int. Ed.* **2010**, *49*, 8598.

(6) (a) Sato, S. *Chem. Phys. Lett.* **1986**, *123*, 126. (b) Irie, H.; Watanabe, Y.; Hashimoto, K. *J. Phys. Chem. B* **2003**, *107*, 5483. (c) Lindgren, T.; Mwabora, J. M.; Avendaño, E.; Jonsson, J.; Hoel, A.; Granqvist, C.-G.; Lindquist, S.-E. *J. Phys. Chem. B* **2003**, *107*, 5709. (d) Asahi, R.; Morikawa, T.; Ohwaki, T.; Aoki, K.; Taga, Y. *Science* **2001**, *293*, 269.

(7) Taflove, A.; Hagness, S. C. *Computational Electrodynamics: The Finite-Difference Time-Domain Method*; Artech House: Boston, 2005.

(8) (a) Christopher, P.; Linic, S. *ChemCatChem* **2010**, *2*, 78. (b) Im, S. H.; Lee, Y. T.; Wiley, B.; Xia, Y. *Angew. Chem., Int. Ed.* **2005**, *44*, 2154.

(9) (a) Govorov, A. O.; Lee, J.; Kotov, N. A. *Phys. Rev. B* **2007**, *76*, No. 125308. (b) Anger, P.; Bharadway, P.; Novotny, L. *Phys. Rev. Lett.* **2006**, *96*, No. 113002.

(10) (a) Yates, J. T., Jr. *Surf. Sci.* **2009**, *603*, 1605. (b) Zhang, Z.; Yates, J. T., Jr. *J. Phys. Chem. C* **2010**, *114*, 3098.